PORTABLE DOSIMETER WITH MOSFET SENSOR FOR RADIOTHERAPY MONITORING

M. A. Carvajal, J. Banqueri, A. J. Palma
Departament of Electronics and Computer Technology, University of Granada, ETSIIT, CITIC-UGR, Granada, Spain

A. M. Lallena
Department of Molecular, Nuclear and Atomic Physics, University of Granda, Granada, Spain

D. Guirado, M. Vilches
Department of Radiophysics, University Hospital San Cecilio, Granada, Spain

Keywords: Radiation sensor, Dosimeter, MOSFET, Radiotherapy, Portable instrument.

Abstract: A portable dosimeter based on unbiased MOSFET sensor is presented. Its main characteristics are an extended linearity range and a notable thermal drift reduction using a unique p-channel MOSFET (pMOS) unbiased during the irradiation period, allowing the location of the sensor without wires for patient comfort and easy-to-use. Both features have been obtained with novel procedures of dose reading and signal processing applied to low-cost commercial pMOS. In this work, a full description of the electronics of the dosimetry system and the signal processing techniques are drawn. The system has been tested with photons from ^{60}Co and the complete technical specifications have been obtained. Among them, we can emphasize: i) dose sensitivity of around 25 mV/Gy; ii) linearity range of more than 50 Gy, with intermediate calibration each 15 Gy, for each sensor; iii) thermal drift below 3 mGy/ºC; iv) resolution below 1cGy; and v) total uncertainty of ± 9 mGy in the temperature range from 19 ºC to 36 ºC . We believe that the proposed dosimeter could be a novel and feasible low-cost alternative to previous commercial dosimetry systems for radiotherapy monitoring in clinical applications.

1 INTRODUCTION

In the last few decades, MOSFETs (Metal-Oxide-Semiconductor Field Effect Transistors) have been used widely as dosimeters due to their small size, immediate and non-destructive readout, low power consumption, easy calibration, and reasonable sensitivity and reproducibility (Holmes-Siedle and Adams, 1986; Hughes et al., 1988; Soubra et al., 1994). These desirable characteristics have promoted the use of this device in different fields such as spacecraft, radiotherapy, skin dosimetry, and clinical monitoring (Buehler et al., 1993; Sarrabayrouse and Siskos, 1998; Benson et al., 2000; Rosenfeld, 2002; Bloemen et al., 2003; Haran et al., 2004; Best et al., 2005; Kwan et al., 2008).

Ionizing radiation produces electron-hole pairs in the MOS structure that are separated by an electric field established in the gate oxide and near the silicon-gate oxide interface. During irradiation, the structure can be configured without an external voltage (*unbiased mode*), or the electric field can be made larger by applying an external voltage between the gate and the bulk of the device (*biased mode*). The charge accumulated in the structure produces changes in the electrical parameters that can be measured experimentally, usually after irradiation, during the so-called readout period. The electrical parameter of the MOS transistors most commonly used as a dosimetric parameter (i.e., the parameter from which the dose is extracted) is the threshold voltage (V_T), which is the gate-source voltage necessary to induce channel inversion between the source and drain terminals. Many works show an approximately linear dependence between the V_T shift and the absorbed dose in the oxide for p-

Carvajal M., Banqueri J., Palma A., Lallena A., Vilches M. and Guirado D..
PORTABLE DOSIMETER WITH MOSFET SENSOR FOR RADIOTHERAPY MONITORING.
DOI: 10.5220/0003128100230029
In *Proceedings of the International Conference on Biomedical Electronics and Devices* (BIODEVICES-2011), pages 23-29
ISBN: 978-989-8425-37-9

channel MOSFETs (pMOS) (Sarrabayrouse and Siskos, 1998; Ma and Dressendorfer, 1989; Hughes et al., 1988).

During readout, the V_T determination can be carried out by extracting the complete current-voltage characteristic curve of the device (Asensio et al., 2006) or by using simpler methods based on constant current measurements. Basically, the measurement methods consist in recording the drain-source voltage while the transistor is being polarized with a constant drain current, before and after irradiation. Under this configuration, the source-drain voltage shifts equals, approximately, the increase in V_T (Sarrabayrouse and Siskos, 1998; Asensio et al., 2006; Carvajal et al., 2010).

Most commercial dosimetric systems based on MOSFETs, measure increases in drain-source voltage at constant drain current (Thomson&Nielsen, 1991; Halvorsen, 2005). Usually, in order to minimize thermal drift, the drain current selected is the Zero Temperature Coefficient, I_{ZTC}, because the drain-source voltage is invariant when temperature increases. The dosimetric parameter used by one of the commercial dosimetric systems is the difference of the increase in drain-source voltages of two transistors under different polarizations. With this arrangement, a wide linear range and thermal compensation are achieved in the biased mode (Thomson&Nielsen, 1991). There is another commercial system based on transistors in the unbiased mode, but the linear range is up to 5 Gy and its use is limited to only one irradiation session (Halvorsen 2005; Sicel Technologies, 2005, Best et al., 2005).

In previous works (Asensio et al. 2006, Carvajal et al., 2010; Carvajal et al., 2010b), we showed the feasibility of using a general-purpose low-cost pMOS as dosimeter, irradiated in unbiased mode, with a significant increase in linear range compared with similar systems and reduced thermal drift. These improvements are based on gate-source voltage measurements at three different drain currents during readout instead of the usual method with a single polarization current.

Although this work has focussed on the pMOS dosimeter, it is important to point out that the proposed methodology could be applied to other sensors based on MOSFET, such as CHEMFET or ISFET, where the magnitude under study is extracted from the threshold voltage. In these cases (Fraden, 1996), the threshold voltage is also measured at constant drain current.

In the following section, a complete measurement system description is carried out, including the measurement algoritmh and an explanation of the electronic system. After this, the experimental setup used in our experiments is described. We report experimental results of the dosimetric characterization of the dosimeter presented here and its technical specifications are shown. Finally, the main conclusions are drawn.

2 DOSIMETER DESCRIPTION

In this section, a detailed description of the measurement algorithm and the electronic design of the dosimeter will be carried out.

2.1 Measurement Algorithm

First, the theoretical background of the measurement process, developed in previous works, will be resumed (Carvajal et al., 2010; Carvajal et al., 2010b). This is the basis on which the electronic design relies on. The operation method of the dose measuring of the presented dosimeter is the same of most previous devices based on MOSFET sensors. Before the sensor irradiation, an electronic reader unit measures the electrical characteristics of the sensor; this is usually named as sensor zeroing (first readout period). Then, sensor is irradiated (irradiation period) and, finally, another readout process is carried out to measure the MOSFET electrical characteristics shifts caused by the irradiation. Here during the irradiation period, we have configured the sensor in *the unbiased mode*, i.e. short-circuiting all its terminals and without polarization, obtaining a sensor without wires in this period.

During the dose readout under constant drain current bias, the gate and the drain terminals of the MOSFET are usually short-circuited and grounded, and the bulk and the source are also inter-connected (Sarrabayrouse and Siskos, 1998; Best et al., 2005). In this configuration, the transistor operates in the saturation region, where $I_D - V_S$ can be modelled for pMOS (Sze, 1981):

$$I_D = \frac{\beta}{2}\left(V_S - |V_T|\right)^2 \quad (1)$$

where the drain current, I_D, depends on the source voltage, V_S, the threshold voltage, V_T, and the β parameter, $\beta = \mu_p C_{ox} \frac{W}{L}$, where μ_p is the carrier mobility in the channel, C_{ox} is the oxide

capacitance, and W and L are the channel width and length respectively.

From Equation (1), the threshold voltage can be calculated before (pre) and after (post) irradiation:

$$|V_t|^{pre} = V_S^{pre} - \sqrt{2I_D}\sqrt{\frac{1}{\beta^{pre}}} \quad (2a)$$

$$|V_t|^{post} = V_S^{post} - \sqrt{2I_D}\sqrt{\frac{1}{\beta^{post}}} \quad (2b)$$

Therefore, the voltage threshold shift can be calculated as follows:

$$\Delta|V_t| = \Delta V_S - \sqrt{2I_D}\left(\sqrt{\frac{1}{\beta^{post}}} - \sqrt{\frac{1}{\beta^{pre}}}\right) \quad (3)$$

If the increase in the source voltage is measured at two different currents, we can write:

$$\Delta|V_t| = \Delta V_{S1} - \sqrt{2I_{D1}}\left(\sqrt{\frac{1}{\beta^{post}}} - \sqrt{\frac{1}{\beta^{pre}}}\right) \quad (4a)$$

and

$$\Delta|V_t| = \Delta V_{S2} - \sqrt{2I_{D2}}\left(\sqrt{\frac{1}{\beta^{post}}} - \sqrt{\frac{1}{\beta^{pre}}}\right) \quad (4b)$$

where ΔV_{Si} is the source voltage shift measured at constant current I_{Di}. Using (4a) and (4b), the threshold voltage shift can be calculated as (Carvajal et al, 2010):

$$\Delta|V_t| = \Delta V_{S1} + \frac{\Delta V_{S2} - \Delta V_{S1}}{1 - \sqrt{\frac{I_{D2}}{I_{D1}}}} \quad (5)$$

With Equation (5), the threshold voltage shifts can be calculated exactly from the source voltage shifts instead of approximated to the source voltage, as has been done until now.

According to equation (5), threshold voltage shifts can be found from voltage increases measured with two different currents, separating the contribution to the source-voltage shifts due to $\Delta\beta$ and $\Delta|V_T|$ and resulting in an extended linear range for the sensor (Carvajal et al, 2010). Moreover, if a third current is applied, a thermal-compensation method and the extension of the linear range can be used simultaneously. Two currents are needed to evaluate equation (5), I_{D1} and I_{D2}, and an additional current, I_C, is required for the thermal compensation of the source voltage shifts measured at I_{D1} and I_{D2} (Carvajal et al., 2010b):

$$\Delta V_{S1}^0 = \Delta V_{S1} + (\Delta V_{SC} - \Delta V_{S1})\frac{\sqrt{I_{D1}} - \sqrt{I_{ZTC}}}{\sqrt{I_{D1}} - \sqrt{I_C}},$$
$$\Delta V_{S2}^0 = \Delta V_{S2} + (\Delta V_{SC} - \Delta V_{S2})\frac{\sqrt{I_{D2}} - \sqrt{I_{ZTC}}}{\sqrt{I_{D2}} - \sqrt{I_C}}, \quad (6)$$

where I_{ZTC} is the current with minimal thermal coefficient of the threshold voltage. According to equation (5), we have:

$$\Delta|V_T^0| = \Delta V_{S1}^0 + \frac{\Delta V_{S2}^0 - \Delta V_{S1}^0}{1 - \sqrt{\frac{I_{D2}}{I_{D1}}}} \quad (7)$$

Evaluating equations (6) and (7) sequentially allows both the thermal compensation and the linearity improvement methods to be taken into account, and provides the thermally compensated threshold voltage shifts from the source-voltage increments measured at three different currents. One need only know the value of I_{ZTC} and the intensities used to polarize the transistor during readout. If one of the currents, I_{D1} or I_{D2}, is equal to I_{ZTC}, equation (7) is simplified. For example, if $I_{D2} = I_{ZTC}$, the source voltage shifts at I_{D2} are thermally compensated, and all that is left is to evaluate equation (7) for ΔV_{S1} and ΔV_C in order to find ΔV_{S1}^0.

Moreover, polarizing with pulsed instead of constant currents, most of the 1/f noise is avoided, obtaining a higher signal-to noise ratio of the measurement (Carvajal et al, 2010).

2.2 Measurement Electronic System

The dosimetric system consists of a read-out unit and a set of sensor modules.

The sensor module is based on the commercial general-purpose pMOS 3N163, which is located on a printed circuit board (PCB). During irradiation and storage periods, all the terminal of the MOSFET must be short-circuited together. In previous works, we used a power supply jack for this purpose, but resulted in a sensor module too thick that could produce radiation shadow areas. For minimizing this effect in the radiation field, the jack was replaced by an n-channel JFET (see Figure 1), with SMD case (surface-mounted-device). We used the MMBF4391 of NXP Semiconductor (Netherland), with a cut off

voltage of -10V and resistance of 30 Ω, and it was welded in the bottom layer of the PCB. This transistor is normally on and maintains connected the source and bulk terminals with the drain and gate. This connection must be opened for zeroing and voltages shifts measurements. Therefore the read-out unit has to provide the adequate source-gate voltage for JFET cut off during the readout process. When the sensor module is removed from the read-out unit, the gate capacitance of the JFET is discharge through a resistor, R_G. Therefore, all the MOSFET terminals are connected again.

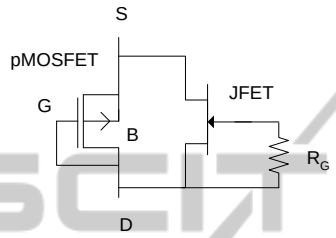

Figure 1: Sensor module schematic.

The readout unit is an electronic system controlled by a microcontroller (Figure 3). We used the PIC-16F877 of the mid-range family of Microchip (USA) due mainly to its low power consumption, its 10 bits analog-to-digital converter (ADC), four independent input/outputs ports and I2C and UART ports. An EEPROM memory is included in order to storage different parameters of each sensor module. One reader unit can support up to 256 different sensor modules. Each sensor module must be identified for zeroing and for dose measurements.

Figure 2: Reader and sensor module.

Figure 3 shows the block diagram of the analog circuitry and the microcontroller. The analog subsystem consists mainly, in a programmable current source, an instrumental amplifier and a digital to analog converter (DAC). During the measurements process of the sensor module, the JFET is cut off, and the programmable source polarizes the MOSFET at different currents, being measured the source voltages by the read-out unit. For zeroing, the microcontroller calculates the DAC output voltage necessary to reduce the instrumental amplifier output down to tens of milivolts. The digitalized source voltages, and the DAC words are storage in the EEPROM, mapped in EEPROM depends on the sensor module identification number, ID. At least, two minutes after the irradiation ends, the dose measurement can be carried out. The sensor ID is introduced in the keypad, and DAC words are restored for each polarization currents. Then, the source voltage source shift can be calculated. The calibration parameters are read from the EEPROM, and the dose are calculated. Finally the results are shown on the display or can be downloaded to the computer.

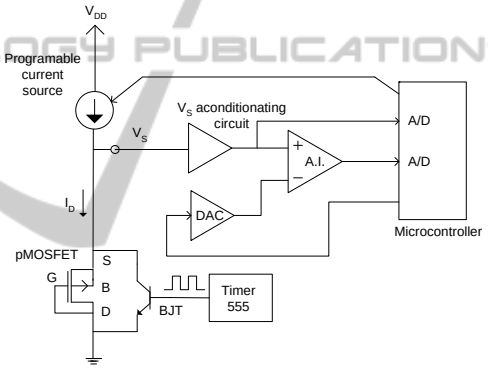

Figure 3: Block diagram of the analog circuitry.

In addition, during the readout process, the pMOS current is switched in order to reduce the 1/f noise and to increase the linearity as Carvajal et al. 2010 shown in a laboratory setup. The collector of a bipolar transistor, the BC547 of NXP Semiconductors (Netherland), is connected to the source of the MOSFET and the emitter is grounded. When the bipolar transistor is activated, the current drains by the BJT, forcing the source voltage of pMOS to zero. But, when the BJT is deactivated, the current crosses the pMOS transistor, and then the source measurement are carried out. The pulse signal was generated with a timer 555. The PWM module of the microcontroller was not used because the PIC was in sleep mode during A/D measurements to reduce the noise produced by the crystal oscillator of the PIC.

The readout unit can be configured by a 4x4 keypad or by computer via the USB port. The results

can be shown on the LCD screen and/or be sent to the PC (Figure 2).

3 EXPERIMENTAL RESULTS

3.1 Experimental Setup

For the evaluation of the presented dosimetry system, a total of eight sensor modules were irradiated with an AECL Theratron 780 located at the University Hospital of San Cecilio in Granada (Spain). This is a teletherapy unit with a ^{60}Co source. All the irradiations were carried out with all four transistor terminals connected to each other, hence without bias voltage, in the 'unbiased' mode. The transistors were irradiated with a 40 x 40 cm^2 field and were placed at the isocentre, at 80 cm from the source. Five transistors were used to study the linearity and measurement range, two for the long-term fading and the last one for short-term fading.

According to a previous work, the three polarization currents included in the dosimeter setup and applied to the sensor during the readout periods were I_{D1} = 30 µA, I_{D2} = I_{ZTC} = 225 µA and I_C = 120 µA . With these current values a thermal drift below 3 mGy/ºC has been obtained (Carvajal et al, 2010b). Moreover, for sensor equalization, an initial pre-irradiation of 30 Gy was necessary.

3.2 Dosimetric Evaluation

In order to evaluate the dosimetric behaviour of the dosimeter, the post-irradiation fading and the linearity range. All these results have been obtained with equations 6 and 7 included in the signal processing.

3.2.1 Post-irradiation Fading

The reordering of the MOSFET charge after the irradiation produces shifts in the dosimetric parameter, i.e. the voltage threshold, which could false the dose reading. This effect is inherent to the transduction principle (measurement of the dose by the charge creation) and very difficulty avoidable. However, what you can do is to characterize it to keep it under control. This has been done with our dosimeter, measuring the short-term fading and the log-term fading to give a time period when both are negligible.

In Figure 4, the short-term post-irradiation fading is shown for several accumulated dose. In this figure, the threshold voltage transient (in arbitrary units) is measured as a function of time.

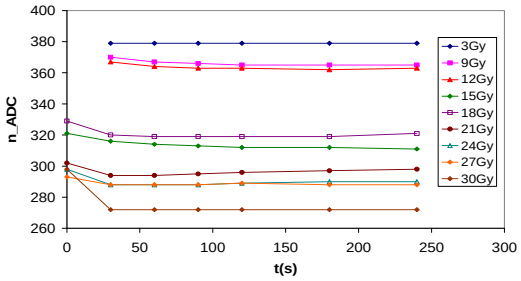

Figure 4: Short-term post-irradiation fading.

From Figure 4, we can observe a measurable transient in the first 60 s and that for long times it is negligible even at higher accumulated dose. The long-term post-irradiation fading was measured every 12 hours, for two sensors with accumulated dose of 27 Gy in 3 Gy sessions. The threshold voltage long-term transients are shown in Figure 5.

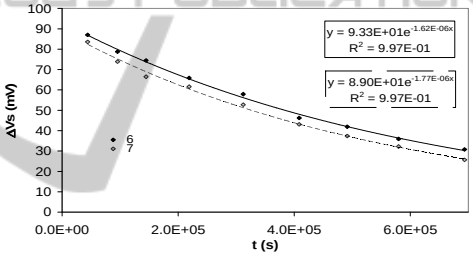

Figure 5: Long-term post-irradiation fading.

From Figure 5, a time constant of around one week was obtained with an exponential fit, in agreement with reported results (Ma and Dressendorfer, 1989). Thus, this dosimeter obtains dose measurements without fading interference at times longer than 60 s and shorter than a few hours after the sensor irradiation. Therefore, we have stated a delay for the measurement between 2 and 3 minutes.

3.2.2 Linearity

One of the disadvantages of using MOSFET sensors in the unbiased mode is the reduced linearity range (Sarrabayrouse and Siskos, 1998). With the readout procedure and the developed instrumentation, this characteristic has been notably improved. Session sensitivities (normalized voltage threshold shift, mV/Gy, per irradiation) are depicted in Figure 6. In Figure 7, the accumulate threshold voltage shifts as a function of the dose up to 52 Gy are shown for five

sensors, where the first 30 Gy have been subtracted and used as pre-irradiation dose for sensor equalization and to improve the sensitivity stability

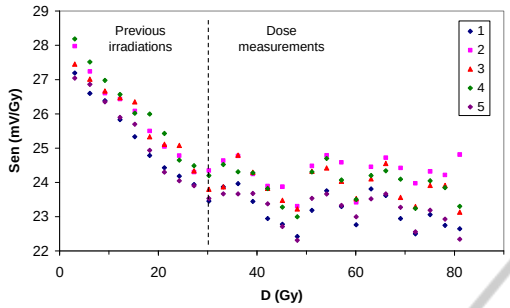

Figure 6: Irradiation session sensitivities versus accumulated dose.

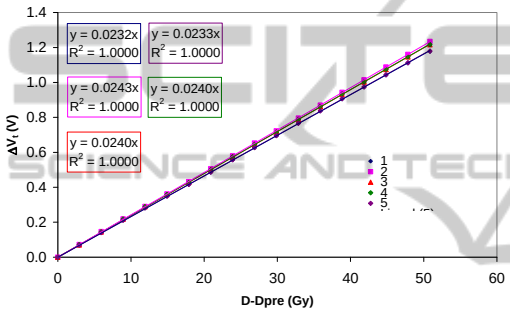

Figure 7: Accumulated threshold voltages shifts versus accumulated dose.

From figures 6 and 7, several remarks can be extracted:

i. A pre-irradiation of 30 Gy is necessary for equalization.
ii. After pre-irradiation, a good linearity is observed
iii. Intervals of accumulated dose of 15 Gy produce linearity errors below 5%
iv. User recalibration every 15 Gy are needed to sure good accuracy for extended linear range up to 52 Gy with a unique sensor.

3.2.3 Technical Specification

In Table 1, the main technical specifications of the presented dosimeter are resumed:

Table 1: Dosimeter technical specifications.

Temperature range	10 – 40 ºC
Resolution	1 cGy
Accuracy	± 3 %
Linear range	15 Gy > 80 Gy*
Thermal drift	< 3mGy/ºC
Delay after irradiation	2 – 3 minutes

* with recalibrations every 15 Gy.

4 CONCLUSIONS

A novel dosimeter based on MOSFET sensor is presented, suitable for radiotherapy monitoring. In the same instrument, main advantages of previous commercial equipment have been joined such us low thermal and fading interference, enough resolution and accuracy for clinical usage, extended linear range and portable reader with wireless sensors. Moreover, these features have been obtained with a low-cost commercial MOSFET instead of expensive and dedicated radiation sensor based on MOS technology.
Regarding with future works, preliminary results with LINAC irradiations (6 and 18 MV) are quite promising. Build-up layer needs to be increased as energy photons increases but general performance is similar to the presented results for Cobalt source.

ACKNOWLEDGEMENTS

This work has been funded by the Ministerio de Educación y Ciencia, Dirección General de Enseñanza Superior (Spain) (Projects CTQ2009-14428-CO2-01, CTQ2009-14428-CO2-02), from the Junta de Andalucía (Projects P09-FQM-5341, P08-FQM-3535) and from the Ministerio de Ciencia e Innovación (Project PS-300000-2009-5).

REFERENCES

Asensio L J, Carvajal M A , López-Villanueva J A, M. Vilches, A. M. Lallena and A. J. Palma, 2006 Evaluation of a low-cost commercial MOSFET as radiation dosimeter *Sensors and Actuators A* 125 288-295,.

Benson C, Joyce M J, O'Connell B and Silvie J 2000 Neutron Detection at the Extremes of Sensitivity in the Cosmic Environment *IEEE Trans Nucl. Sci.* 6 2417-2422.

Best S, Ralson A and Suchowerska N 2005 Clinical Application of the OneDose™ Patient Dosimetry System for total body irradiation *Phys. Med. Biol.* 50 5909-5919.

Bloemen E, Bois W, P. Visser P, Bruinvis I, Jalink D, Hermans J and Lambin P 2003 Clinical dosimetry with MOSFET dosimeters to determinate the dose along the field junction in a split beam technique *Radiother. Oncol.* 67 (2003) 351-357.

Buehler M G, Blaes B R, Soli G A and Tardio G R 1993 On Chip p-MOSFET Dosimetry *IEEE Trans. Nucl. Sci.* 40 1442-1449.

Carvajal M A, Vilches M, Guirado D, Lallena A M, Banqueri J and Palma A J, 2010 Readout techniques for linearity and resolution improvements in MOSFET dosimeters *Sensors and Actuators A* 157 178–184.

Carvajal M A, Martínez-Olmos A, Morales D P, López-Villanueva J A, Lallena A M and Palma A J, 2010 Thermal Drift Reduction With Multiple Current Polarization For MOSFET Dosimeters send for publication to *Phys. Med. Biol.*

Fraden J, 1996 *Handbook of modern sensor. Physics, design and application, 2nd Edition* (New York: Springer Science+Biseness Media).

Halvorsen P. H. 2005. Dosimetric evaluation of a new design MOSFET in vivo dosimeter, *Med. Phys.* 32 110-117.

Haran A, Jaksic A, Refaeli N, Eliyahu A, David D and Barak J 2004 Temperature Effects and Long Term Fading of Implanted and Unimplanted Gate Oxide RADFETs, *IEEE Trans. Nucl. Sci.* 5 2917-2921.

Holmes-Siedle A and Adams L 1986 RADFET: A review of the use of metal-oxide-silicon devices as integrating dosimeters *Radiat. Phys. Chem.* 28 235-244.

Hughes R C, Huffman D, Snelling J V, Zipperian J E, Ricco A J and Kelsy A 1988 Miniature Radiation Dosimeter for In-Vivo Radiation Measurements, *Int. J. Radiat. Oncol. Biol. Phys.* 14 963-967.

Kwan I S, Rosenfeld A B, Qia Z Y, Wilkinson D, Lerch M L F, Cutajar D L, Safavi-Naeni M, Butson M, Bucci J A, Chin Y and Perevertaylo V L 2008 Skin dosimetry with newMOSFET detectors *Radiation Measurements* 43 929 – 932.

Ma T P and Dressendorfer P V 1989 *Ionizing Radiation Effects In MOS Devices and Circuits* (New York: John Wiley & Sons).

Rosenfeld A B 2002 MOSFET Dosimetry on Modern Radiation Oncology Modalities, *Radiat. Prot. Dosim.* 101 393-398.

Sarrabayrouse G and Siskos S 1998 Radiation Dose Measurement using MOSFETs, *IEEE Instrum. Meas. Mag.* 1 26-34.

Soubra M, Cygler J and Mackay G 1994 Evaluation of a dual bias metal oxide-silicon semiconductor field effect transistor detector as radiation dosimeter, *Med. Phys.* 21 (1994) 567-572.

Sicel Technologies 2005 OneDose User´s Manual, Pre-production draft version, rev. P01, (Morrisville: Sicel Technologies Inc.).

Sze S M 1981 *Physics of Semiconductor Devices, 2nd edition.* (New York: John Wiley & Sons)

Thomson & Nielsen 1991 Direct reading dosimeter *European Patent Office* EP 0471957A2, (02/07/1991).